Surface plasmon polariton modified emission of erbium in a metallodielectric grating

J. Kalkman,[a] C. Strohhöfer, B. Gralak, and A. Polman
FOM-Institute for Atomic and Molecular Physics, Kruislaan 407, 1098 SJ Amsterdam, The Netherlands

(Received 20 February 2003; accepted 2 May 2003)

The spectral shape and bandwidth of the emission of Er^{3+} ions in silica glass around 1.5 μm is strongly modified by the presence of a silver grating. The metallodielectric grating was made by a sequence of ion implantation in silica glass, dry etching, and silver sputter deposition. Spectral enhancements are observed that are attributed to near-field coupling of Er^{3+} ions to surface plasmon polaritons that subsequently reradiate at well-defined resonance conditions. Qualitative agreement is observed between these resonance conditions and calculations based on the surface plasmon polariton dispersion relation. © *2003 American Institute of Physics.* [DOI: 10.1063/1.1589198]

Erbium ions play a key role in optical communication systems operating at 1.5 μm. The 1.5 μm emission is due to radiative intra-$4f$ transitions that occur between the $^4I_{13/2}$ and $^4I_{15/2}$ manifolds of Er^{3+}. These manifolds are composed of a multitude of Stark levels, the number of which is determined by the site symmetry of the Er ion in the host. The absorption and emission spectra of Er are thus determined by Boltzmann distributions over the ground and excited manifolds and, hence, at a certain temperature the Er emission spectrum is fixed for a given material. Many of the applications of Er-doped materials depend critically on the exact line shape of the emission. For example, in wavelength-division multiplexing systems, the systems bandwidth is determined by the width of the spectrum. Hence, it would be extremely interesting if the Er emission spectrum could be externally modified. In this letter we show that a spectacular change in the emission spectrum of Er-doped silica glass can be achieved by coupling Er ions to surface plasmon polaritons (SPPs) in a metallodielectric grating.

Heraeus silica glass slides (Herasil 1) of 500 μm thickness were cooled to 77 K and implanted with 1.2×10^{15} Er/cm^2 at an energy of 350 keV. The ion range and straggle are 120 and 35 nm, respectively, as measured by Rutherford backscattering spectrometry. An optical grating was then fabricated in the implanted face of the silica glass by electron beam lithography and dry etching. The samples then were annealed at a temperature of 800 °C for 1 h in vacuum to increase the luminescence yield of the implanted Er.[1] Next, a silver layer was sputter deposited onto the grating. From optical diffraction as well as reflectivity measurements and accompanying calculations based on the numerical method of exact eigenvalues and eigenfunctions[2] the structural parameters of the silver grating were determined: depth 230 ± 10 nm, pitch 1070 ± 1 nm, and width of the silver grating bars 500 ± 10 nm. Cross-section scanning electron microscopy showed good conformity and adhesion of the Ag film on the grating, i.e., the silver was found to be in contact with the silica throughout the entire cross section of the grating. The silver layer thickness was 300 nm, i.e., thicker than the depth of the grating. In this way a metallic grating with a dielectric top layer was made, where the dielectric acts as a host and a spacer for the Er^{3+} ions above the grating (see schematic in Fig. 1).

Photoluminescence (PL) measurements were performed at room temperature. An argon-ion laser operating at 488 nm was used to excite the Er^{3+} ions into the $^4F_{7/2}$ manifold. The laser light was modulated by an acousto-optical modulator and fed into a polarization maintaining fiber. The fiber axis was aligned with the polarization direction of the laser light such that light at the output of the fiber was polarized with an *s* over *p* intensity ratio of at least 30. The output of the fiber was focused from the silica side onto the grating (see schematic Fig. 1) using a microscope objective (spot diameter ~ 700 μm). The fiber was mounted at an angle of 45° relative to the surface normal onto the rotating sample stage, thereby keeping the excitation angle fixed during rotation (the corresponding internal angle in the silica glass is 29°). The excitation power at the sample was measured at the exit of the pump fiber with a Si photodiode. PL was collected by an $f=10$ cm lens and filtered by a long-pass filter ($\lambda > 846$ nm) to remove any intensity left from the pump. The in-plane collection angle was 16°. PL was analyzed with an infrared polarizer and dispersed with a 480 mm focal-length monochromator. The resolution was 6 nm. The collected PL was detected by a liquid-nitrogen cooled Ge diode in combination with a standard lock-in technique.

Figure 1 shows normalized PL spectra taken at various angles relative to the surface normal (angle θ in the schematic and insets). Data are shown for the two orientations of the grating as shown by the insets in the figure. In Fig. 1(a) the grating vector **G** is in the plane of measurement ($\mathbf{G}_\parallel$) and only data for *p*-polarized emission is plotted. At $\theta=40°$ an emission spectrum characteristic for Er^{3+} in bulk silica glass is observed. At $\theta=20°$ only a slightly different spectral shape is observed. However at $\theta=0°$, a strongly increased spectral contribution compared to that of Er^{3+} in bulk silica glass is observed for the long wavelength part of the spectrum ($\lambda > 1530$ nm). In Fig. 1(b) **G** is perpendicular to the plane of measurement ($\mathbf{G}_\perp$) and only data for *s*-polarized emission are plotted. Here for all angles well-defined peaks are observed, superimposed on the spectrum for Er^{3+} in bulk silica

[a]Electronic mail: j.kalkman@amolf.nl

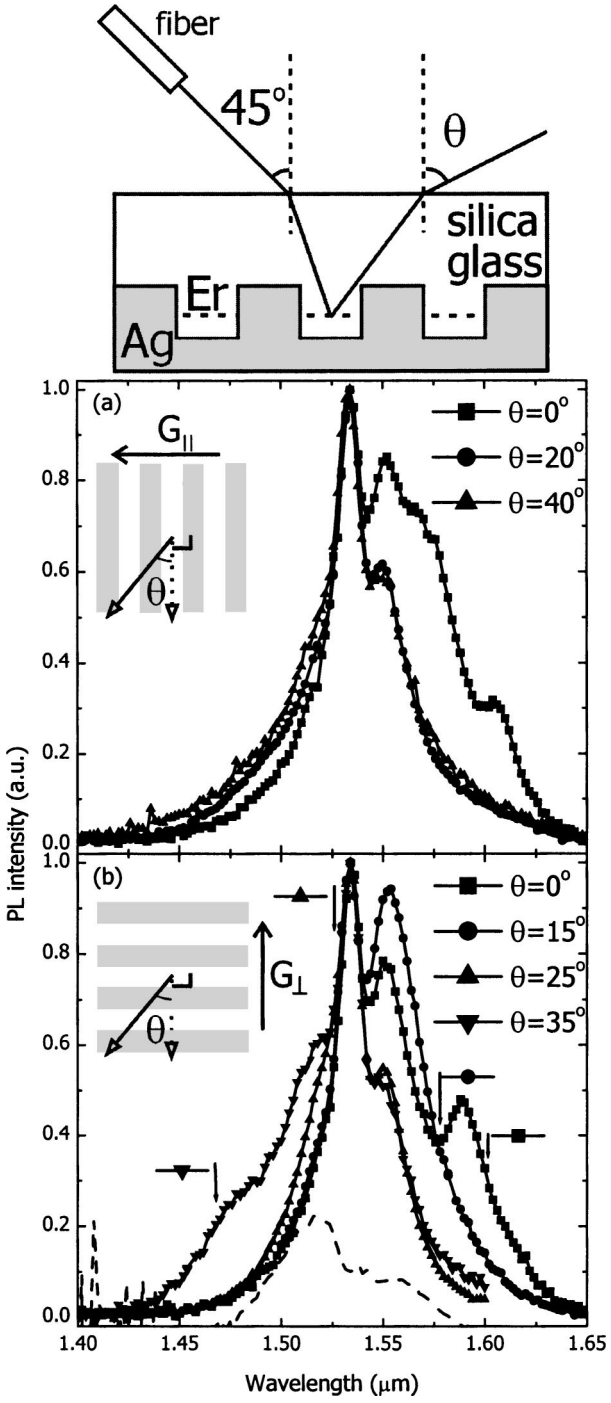

FIG. 1. PL of Er-doped metallodielectric gratings measured at various angles θ [see schematic of measurement geometry and insets in (a) and (b)]. (a) $\mathbf{G}_{\parallel}$; data for *p*-polarized emission; (b) $\mathbf{G}_{\perp}$; data for *s*-polarized emission. The arrows in (b) indicate the measured peak wavelength of the contribution of the reradiated SPPs for each angle. For $\theta=25°$ the dashed line shows a spectrum that was obtained by dividing the measurement by a reference spectrum, showing the enhancement in PL at the position of the arrow.

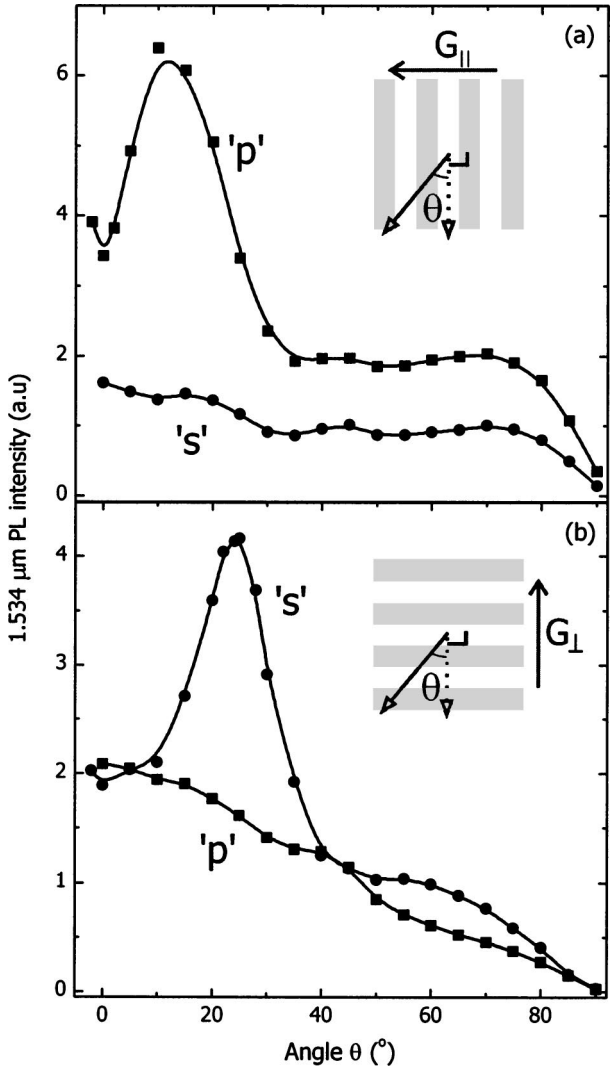

FIG. 2. PL intensity as a function of θ for both *s* and *p* polarization. (a) $\mathbf{G}_{\parallel}$; (b) $\mathbf{G}_{\perp}$.

glass. The peak wavelength decreases with increasing angle.

Figure 2 shows the PL intensity at a fixed wavelength of 1.534 μm as a function of angle for *s* and *p* polarization. Figure 2(a) shows data for $\mathbf{G}_{\parallel}$. A clear PL enhancement is observed around $\theta=10°$ for *p*-polarized emission. No enhancement is observed for *s*-polarized PL. In Fig. 2(b) the opposite is observed. It shows data for $\mathbf{G}_{\perp}$ where an enhancement is observed around $\theta=25°$ for *s*-polarized PL. No enhancement is observed for *p*-polarized PL.

The enhancements observed in Figs. 1 and 2 are attributed to reradiating SPPs that couple out at well-defined resonance conditions. The SPPs are excited by the near field of the Er^{3+} ions and propagate in all directions along the interface. The normally nonradiative SPP can radiate into the far field by diffraction on the grating. The observed spectrum in Fig. 1 is then a linear superposition of the spontaneous emission spectrum for Er^{3+} in bulk silica glass and the reradiated SPPs collected at the measurement angle. The enhancements in Fig. 2 show the angles at which a reradiated SPP occurs if it is excited at an energy corresponding to 1.534 μm. Since the damping distance of the propagating SPP is estimated to be of the order of 100 μm (calculated at 1.5 μm for a planar interface), i.e., many grating periods, the peaks in Fig. 2 are expected to be very sharp. The fact that in Fig. 2 a relatively broad width is observed is due to the relatively large collection angle that was used in these measurements. Reference measurements were performed on samples from the same Er^{3+} doped silica glass slide either covered with a planar silver mirror or not covered (air). These only show a gradual decrease of PL with angle comparable to that for *s*-polarized light in Fig. 2(a) and *p*-polarized light in Fig. 2(b). This

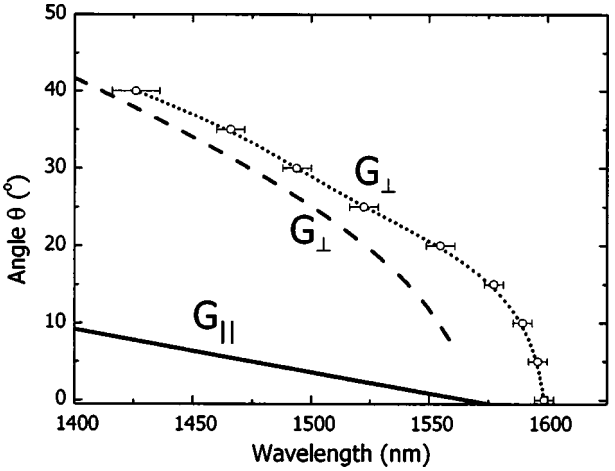

FIG. 3. Resonance angles for SPP reradiation for the two grating orientations calculated from the dispersion relation, Snell's law and Eq. (1); $\mathbf{G}_{\|}$ (solid line) and $\mathbf{G}_{\perp}$ (dashed line). For $\mathbf{G}_{\perp}$ the measured peak wavelengths, derived from the data in Fig. 1(b), are shown (open circles). The dotted line is a guide for the eye.

gradual decrease in PL for increasing emission angle is due to the increasing internal reflection coefficient of the SiO_2/air interface as well as the decreasing internal collection angle. Note also that due to refraction at the SiO_2/air interface the maximum internal angle at which light from the grating is detected is 44°, the angle of total internal reflection at the SiO_2/air interface.

To quantitatively analyze the data, the optical constants of both the Ag film and silica glass substrate were measured with spectroscopic ellipsometry. We found $\epsilon_{\text{silica}}=2.1$ and $\epsilon_{\text{Ag}}=-98.07+6.95i$ at 1.5 μm. Using these data the dispersion relation for a SPP propagating along a planar Ag/SiO_2 interface was calculated. For arbitrary grating orientation conservation of the tangential component of the wave vector leads to the resonance condition

$$\mathbf{k}_{0\|}=\pm\mathbf{k}_{\text{SPP}}\pm m\mathbf{G}, \tag{1}$$

where $\mathbf{k}_{0\|}$ is the projection of the photon wave vector in the silica glass onto the interface ($|\mathbf{k}_{0\|}|=|\mathbf{k}_0|\sin\theta_{\text{int}}$, θ_{int} being the internal angle of the photon relative to the surface normal), $\mathbf{k}_{\text{SPP}}$ is the SPP wave vector, $\mathbf{G}$ is the grating vector, and m is an integer. Since $k_{\text{SPP}}>k_{0\|}$ one or more grating vectors must be added or subtracted from the SPP wave vector to obey the resonance condition, leading to the enhanced PL. For the sample geometry studied only the resonance for $m=1$ is observed as the higher order resonances occur at $\theta_{\text{int}}>44°$, for which external collection is obscured by total internal reflection at the SiO_2/air interface. With Eq. (1), the SPP dispersion relation, and Snell's law the external angle θ was calculated at which a reradiated SPP occurs in the PL spectrum if it was excited at frequency ω. To facilitate qualitative comparison with the data these angles are plotted versus vacuum wavelength in Fig. 3. The calculated angles are shown in Fig. 3 by the dashed line for the $\mathbf{G}_{\perp}$ case.

We can now compare these data with the peak wavelengths observed in Fig. 1(b). Exact values for the peak wavelengths were determined by dividing the PL spectra in Fig. 1(b) by the PL spectra measured for Er^{3+} in silica glass above a planar silver mirror (see, e.g., dashed line in Fig. 1(b) for $\theta=25°$). These are indicated by arrows in Fig. 1(b) and are also plotted as a function of angle in Fig. 3 (open circles). Clearly the same gradual trend of decreasing angle with increasing wavelength is observed in both the experimental data and calculations. The error in the determination of the peak wavelength becomes larger for smaller wavelengths due to a decrease in intensity and an increase of the width of the enhancement. Experimentally, for all wavelengths the coupling occurs at a larger angle than found in the calculation. This can be understood from the fact that the calculation is done for a planar interface, rather than the actual structure, a corrugated interface. Indeed surface corrugation changes the SPP dispersion relation in a way that leads to an increased SPP wave vector,[3] and thus to an increased resonance angle for a particular wavelength, as is observed.

Figure 3 also shows a calculation for $\mathbf{G}_{\|}$ (solid line) that shows much less change of the angle at which the SPP reradiates versus wavelength. From these calculations we only expect enhancements in the Er^{3+} emission spectrum for angles between 0° and 10°. As here too, surface corrugation leads to an increased resonance angle compared to the case for a planar film, the calculation is in qualitatively agreement with the data in Figs. 1(a) and 2(a). The polarization dependence observed in Fig. 2 is in agreement with data by Kitson *et al.*,[4] who have measured the polarization-dependent emission of a dye above a sinusoidal Ag grating. Also, photoacoustic measurements by Inagaki *et al.*,[5] showed similar polarization dependence in reflection.

These data demonstrate the use of Er ions as a source for infrared SPPs at the important 1.5 μm telecommunication wavelength. Because SPPs in the infrared have large propagation lengths they could be used in two-dimensional-plasmon optics experiments.[6] In contrast to what is typically observed with dyes[4] and rare earth complexes,[7] Er ions in silica glass show no photo bleaching. The long lifetime of Er in silica glass (and, hence, a high quantum efficiency) enables the study of radiative and nonradiative components in the Er–SPP coupling.

In summary we have shown a significant modification of the photoluminescence spectrum of Er^{3+} in silica glass by coupling to surface plasmon polaritons in a metallodielectric grating, which subsequently reradiate at well-defined resonance conditions. The spectral enhancements are in qualitative agreement with a model based on the SPP dispersion relation that was calculated using experimentally determined dielectric constants. These results may lead to various applications in infrared plasmon optics.

This work is part of the research program FOM and was made possible by financial support from NWO.

[1] A. Polman, D. C. Jacobson, D. J. Eaglesham, R. C. Kistler, and J. M. Poate, J. Appl. Phys. **70**, 3778 (1991).
[2] L. Li, J. Mod. Opt. **40**, 553 (1993).
[3] I. Pockrand, Phys. Lett. **49A**, 259 (1974).
[4] S. C. Kitson, W. L. Barnes, and J. R. Sambles, Opt. Commun. **122**, 147 (1996).
[5] T. Inagaki, J. P. Goudonnet, and E. T. Arakawa, J. Opt. Soc. Am. B **3**, 992 (1986).
[6] H. Ditlbacher, J. R. Krenn, G. Schider, A. Leitner, and F. R. Aussenegg, Appl. Phys. Lett. **81**, 1762 (2002).
[7] P. Andrew and W. L. Barnes, Phys. Rev. B **64**, 125405 (2001).